

Bone Morphogenetic Protein-2 Binds As Multilayers To A Collagen Delivery Matrix: An Equilibrium Thermodynamic Analysis

Randy Morin,[†] David Kaplan,[‡] and Bernardo Perez-Ramirez^{*,†}

Formulation and Process Development, Wyeth BioPharma, One Burt Road, Andover, Massachusetts 01810, and Department of Biomedical Engineering & Chemical and Biological Engineering, Tufts University, 4 Colby Street, Medford, Massachusetts 02155

Received July 1, 2005; Revised Manuscript Received October 14, 2005

Recombinant human bone morphogenetic protein-2 (rhBMP-2) promotes bone growth but must be retained at the delivery site for optimal efficacy *in vivo*. rhBMP-2 release from a collagen-based matrix has shown favorable pharmacokinetics. The present study assessed binding affinity and binding saturation of rhBMP-2 to a collagen matrix as a function of solution and rhBMP-2 isoform variables. Results indicate that rhBMP-2 binds to the collagen matrix with affinities on the order of 10^3 to 10^4 M⁻¹. Maximum binding, ν , was primarily a function of pH for heterogeneous rhBMP-2 and the extended (T₂₆₆/T₂₆₆) isoform. However, binding saturation of the <Q₂₈₃/<Q₂₈₃ isoform was unaffected by pH. Overall, binding saturation was higher than the calculated saturation of a rhBMP-2 monolayer, suggesting both hydrophobic and ionic interactions in a multilayer formation. The contributions of pH and ionic strength to the linkage free energy of interaction was on the order of 1.3 kcal mol⁻¹ and ~0.3 kcal mol⁻¹, respectively. This thermodynamic approach can serve to optimize interactions between therapeutic proteins and delivery systems.

Introduction

Purified collagen is ubiquitous in biomedical applications. Collagen has low immunogenicity, induces homeostasis,¹ and can be processed into a number of forms, such as sheets, tubes, sponges, powder, and injectable solutions, all of which have applications in the medical field.² The mechanical integrity and biodegradation of collagen are easily controlled by chemical cross-linking. Additionally, chemical modification of amino groups in the conserved structure of collagen has been used advantageously to control drug release from its surface.^{3,4} As a consequence of the scaffolding properties and the effect on cellular activity, collagen-based sponge matrixes play an important role in tissue engineering research in combination with growth factors. Coating of a collagen sponge with basic fibroblast growth factor facilitates early dermal and epidermal wound healing.⁵ Besides dermal wound healing, another major field for application of collagen is scaffolds in conjunction with therapeutic proteins such as recombinant bone morphogenetic protein 2 (rhBMP-2).^{6–9} Depending on the application site, rhBMPs seem to influence both endochondral and intramembranous bone formation pathways by mesenchymal cell recruitment and differentiation.¹⁰ Similar influences are observed *in vitro*, related to tissue-specific outcomes.^{11,12}

The rhBMP-2 protein is a member of the transforming growth factor- β (TGF- β) super family and is used as a powerful adjuvant for bone regeneration in surgical procedures^{9,13} where significant amounts of bone are absent or removed. Specifically, rhBMP-2 induces bone by signaling for differentiation of

progenitor cells into osteoblasts¹⁴ and by up-regulation of mRNA coding for myriad proteins including α 1(I) collagen.¹⁵ Recombinant production of rhBMP-2 initially yields a translated 396-amino-acid precursor propeptide. Subsequent N-terminal digestion by a coexpressed enzyme cleaves the first 282 amino acids, resulting in a mature rhBMP-2 monomer, or the first 265 amino acids, resulting in an extended monomer.¹³ Thus, the rhBMP-2 monomers of each dimer are composed of either 114 amino acids with a glutamine (Q₂₈₃) N-terminus or 131 amino acids with a threonine (T₂₆₆) N-terminus (the numbers for these amino acids indicate their position in the propeptide, i.e., Q₂₈₃ and T₂₆₆ are at position 1 in the mature and extended monomers, respectively). In solution, the N-terminus of a glutamine monomeric unit can cyclize to form pyroglutamic acid (<Q₂₈₃). These three rhBMP-2 monomeric units combine to form 6 covalent dimers in solution denoted as <Q₂₈₃/Q₂₈₃, <Q₂₈₃/Q₂₈₃, Q₂₈₃/Q₂₈₃, <Q₂₈₃/T₂₆₆, Q₂₈₃/T₂₆₆, and T₂₆₆/T₂₆₆.¹³

The success of rhBMP-2 in eliciting bone regeneration *in vivo* depends on extended residence time at the surgical site.^{6–8} It has been shown that rhBMP-2 requires combination with a biomaterial matrix to attain maximal efficacy.^{9,16–18} Ideal delivery matrixes are characterized by adequate porosity to allow cell and blood vessel infiltration, appropriate mechanical stability against compression and tension, and biocompatibility and biodegradability.⁹ Collagen sponges have been under investigation as scaffolds in the emerging field of tissue engineering and, more specifically, as delivery systems for rhBMP-type molecules. The binding and slow release profile of rhBMP-2 from a collagen sponge yields an optimum pharmacokinetic profile for *in vivo* bone regeneration in comparison to other delivery matrixes.⁹ Prior studies have addressed the interaction of rhBMP-2 and collagen sponges.^{19–21} However, this is the first description of using equilibrium thermodynamics to elucidate the contribution of solution variables to rhBMP-2 binding to collagen. A similar study has been performed recently on the

* Correspondence to Bernardo Perez-Ramirez at his present address: BioFormulations Development, Genzyme Corporation, 1 Mountain Road, Framingham MA 01701. Telephone 508-270-2117, E-mail: bernardo.perez@genzyme.com.

[†] Wyeth BioPharma.

[‡] Tufts University.

adsorption of rhBMP-2 onto hydroxyapatite.²² The objective of the present study was to clarify and quantify the interaction(s) between a collagen matrix and rhBMP-2. Toward this objective, the following questions were addressed. First, what is the nature of the interaction between the rhBMP-2 and the collagen matrix in terms of surface layers and interactions? Second, what are the effects of solution variables on the rhBMP-2 collagen interactions? Third, what is the impact of the rhBMP-2 isoforms in binding to the collagen matrix? The results of these investigations are the subject of this paper. These data provide a more rational basis for optimization of rhBMP-2 collagen matrix loading to enhance future therapeutic impact.

Materials and Methods

Materials. The stock rhBMP-2 was produced by Wyeth Biopharma, Andover MA at 4.7 mg/mL in 5 mM L-glutamic acid, 5 mM NaCl, 2.5% w/v glycine, and 0.5% w/v sucrose at pH 4.5, following a published procedure.²³ Collagen matrixes were purchased as 3 in × 4 in Helistat absorbable collagen type-I sponges manufactured by Integra Life Sciences Corporation in Plainsboro, NJ. Collagen cylinders were cut from the absorbable collagen sponges using a Uni-Punch disposable biopsy punch from Premier Medical Products.

Collagen Matrix Preparation. Collagen cylinders were cut to diameters of 3 mm or 4 mm from Helistat sponges. The collagen content of the cylinders was approximated as the average dry mass of the cylinders. The dry mass of the collagen cylinders was determined by thermogravimetric analysis²⁴ (TA Instruments, model TGA 2050). Several sets of three cylinders from three different collagen sponges were tested. The overall average dry mass of a collagen cylinder was found to be approximately 88% of the ambient mass of the collagen cylinder. For the 4 mm collagen cylinders, the highest experimentally determined dry mass was 0.76 mg.

All collagen cylinders in subsequent binding experiments were first centrifuged at 4 000 rpm, in a SS-34 Sorvall rotor in selected buffers for up to 60 min in order to expel any air pocket inside the matrix. Binding equilibrium was assessed in two different buffers. The first buffer contained 5 mM L-glutamic acid and no added NaCl at pH 4.4. The second buffer contained 5 mM L-glutamic acid and 25 mM NaCl at pH 5.4. Binding strength was evaluated in nine different buffers, each with 5 mM L-glutamic acid; 12 mM, 25 mM, or no added NaCl; and at pH 4.5, 4.9, or 5.4. Then, the cylinders were gently stirred in large volumes of the selected buffer overnight at 2–8 °C to dialyze out any residual ions trapped inside the matrix. A preliminary experiment was conducted to determine the average buffer volume transferred from the saturated collagen cylinders to the samples. This average transfer volume was accounted for in final calculations.

rhBMP-2 as Ligand. The rhBMP-2 used in these binding experiments was first dialyzed against three 24-h exchanges of 100× volumes of selected buffer at 2–8 °C (8 000 MWCO Spectra/Por dialysis tubing from Spectrum). The dialysate NaCl concentration was determined using a Hamilton PRP-X250 anion exchange column and indirect UV chromatographic quantitation of chloride as previously described.^{25,26} The rhBMP-2 concentration was determined by UV absorbance at 280 nm, using an absorptivity value of 1.43 [mL/(mg cm)], before subsequent dilutions with corresponding buffer. The result was a series of rhBMP-2 concentrations, ranging from 20 to 750 µg/mL, in buffer at selected pH values and NaCl concentrations. For experiments measuring the binding between collagen cylinders and the rhBMP-2 isoforms, the <Q₂₈₃/Q₂₈₃ and T₂₆₆/T₂₆₆ isoforms were first purified by cation exchange chromatography following published procedures,^{19,27} slightly modified. Specifically, the isoforms were separated using a Pharmacia Mono S, 5.0 mm × 50 mm column with an initial mixture of 85% A phase (20 mM sodium acetate, 10% acetonitrile, pH 5.0), 15% B phase (20 mM sodium acetate, 1.5 M NaCl, 10% acetonitrile), and a final mixture of 30% A phase and 70% B phase.²⁶

Evaluation of Binding Equilibrium. An initial set of experiments was conducted to determine the minimum time required for the binding to reach equilibrium. Only the extreme rhBMP-2 concentrations, buffer pH, and buffer ionic strength that would be used in subsequent binding experiments were sampled. Specifically, stock rhBMP-2 was dialyzed into one of two buffers. Briefly, as noted above, the first buffer contained 5 mM L-glutamic acid and no added NaCl and was titrated to pH 4.4 with NaOH. The second buffer contained 5 mM L-glutamic acid and 25 mM NaCl and was titrated to pH 5.4 with NaOH. The rhBMP-2 titrated into these two buffers was diluted to concentrations of 750 µg/mL and 20 µg/mL. Additionally, control samples with no rhBMP-2 were prepared in both buffers for a total of six conditions.

Either three saturated 3-mm collagen cylinders or three saturated 4-mm cylinders, or the average saturation volume (control), was placed into each of the six conditions. The resulting eighteen samples were prepared in duplicate and incubated at 25 °C with gentle motion. Small volumes were taken at 6, 25, 45, 68, and 116 h and frozen at –80 °C for subsequent quantitation and analysis.

Evaluation of Binding Strength. To measure binding strength as a function of ionic strength and pH, binding experiments were performed with buffers consisting of, as noted above, 5 mM L-glutamic acid; 12 mM, 25 mM, or no added NaCl; and titrated to pH 4.5, pH 4.9, or pH 5.4. One saturated 4-mm collagen cylinder was placed into each of 4 mL in a series of twelve rhBMP-2 concentrations between 0 µg/mL and 750 µg/mL. Controls consisted of rhBMP-2 diluted to the same rhBMP-2 concentrations with the addition of the saturation volume instead of a collagen cylinder.

The resulting 108 conditions were prepared in duplicate for samples and controls and placed into a 25 °C water bath shaken slowly at 60 strokes per minute for 72 h. The rhBMP-2 concentration remaining free in solution after 72 h was determined by reverse-phase HPLC.²⁰

Bound rhBMP-2 was calculated as the difference between initial rhBMP-2 and free rhBMP-2 remaining at 72 h. Apparent equilibrium binding constants, described as K_b , were approximated from the negative slopes of Scatchard plots. In the case of curvilinear Scatchard plots, equilibrium binding constants, described as K_{b1} and K_{b2} , were calculated from the slopes of tangent lines to the two phases of the curvilinear plot. Binding saturations, described as ν , were calculated from the x-intercept of the lines in the Scatchard plots.

Statistics. Plots were generated using Microsoft Excel software. Where error bars are present, data points represent the mean of two samples and error bars represent the standard deviation (SD) of those two samples, as determined by the Excel software. Where error bars are absent, data points represent a single sample.

Results

Calculated Limits of rhBMP-2 Occupancy in the Collagen Matrix. Theoretical calculations were performed using the simplest scenarios possible to determine the low and high limits of binding saturation, namely, ν , of the collagen delivery system with rhBMP-2. A theoretical low limit of ν was calculated as the mass of rhBMP-2 that binds in a saturated monolayer to the total surface area of a collagen matrix as determined by Brunauer–Emmett–Teller (BET) analysis.²⁶ A theoretical high limit of ν was calculated as the mass of rhBMP-2 that fully occupies the free volume in the collagen matrix. Figure 1 shows a diagram of the low limit of total surface saturation and the high limit of free volume saturation of rhBMP-2 occupancy in the matrix of the collagen cylinder.

Low Limit of ν : rhBMP-2 Saturation on the Matrix Surface inside the Collagen Cylinder. The theoretical saturation limits are based on rhBMP-2 dimer dimensions of 70 Å × 35 Å × 30 Å²⁸ and assume no change upon adsorption. Depending on the orientation of the dimer to the surface, the minimum area

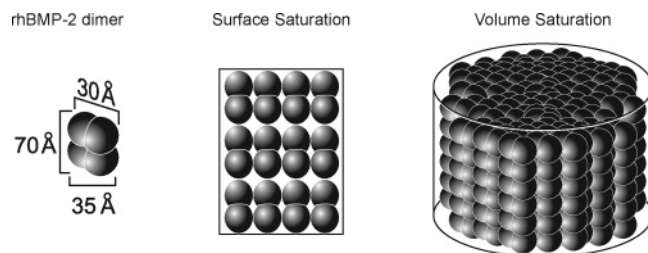


Figure 1. Schematic of rhBMP-2 and collagen interactions as surface saturation and volume saturation.

occupied by a single rhBMP-2 molecule is 1050 \AA^2 ($30 \text{ \AA} \times 35 \text{ \AA}$), while the maximum area occupied is 2450 \AA^2 ($70 \text{ \AA} \times 35 \text{ \AA}$). Thus, the minimum and maximum areas occupied by a single rhBMP-2 molecule are therefore 1.05×10^{-17} and $2.45 \times 10^{-17} \text{ m}^2$, respectively. BET analysis revealed the collagen matrix to have a total surface area of approximately $2.4 \times 10^{-3} \text{ m}^2/\text{mg}$.²⁶ Hence, the low limit of the monolayer saturation of rhBMP-2 on the surface of 1 mg of collagen matrix is 9.80×10^{13} molecules/mg ($2.4 \times 10^{-3} \text{ m}^2/\text{mg}$ per $2.45 \times 10^{-17} \text{ m}^2/\text{molecule}$), if each rhBMP-2 dimer occupies the largest area possible, and 2.29×10^{14} molecules/mg ($2.4 \times 10^{-3} \text{ m}^2/\text{mg}$ per $1.05 \times 10^{-17} \text{ m}^2$), if each rhBMP-2 dimer occupies the smallest area possible.

Using Avogadro's number, i.e., 6.022×10^{17} molecules/ μmol and a nominal relative molecular mass, M_r , for rhBMP-2 of 30 000, the monolayer saturation of rhBMP-2 on the two-dimensional surface area of the collagen matrix is $4.9 \mu\text{g}$ rhBMP-2/mg collagen matrix (9.8×10^{13} rhBMP-2 molecules/mg collagen matrix $\times 1 \mu\text{mol}/6.0228 \times 10^{17}$ molecules $\times 30,000 \mu\text{g}/1 \mu\text{mol}$) for rhBMP-2 presenting maximum surface area to the collagen surface and $11.0 \mu\text{g}$ rhBMP-2/mg collagen matrix (2.29×10^{14} rhBMP-2 molecules/mg collagen $\times 1 \mu\text{mol}/6.0228 \times 10^{17}$ molecules $\times 30,000 \mu\text{g}/1 \mu\text{mol}$) for rhBMP-2 presenting minimum surface area to the collagen surface. Therefore, on the basis of the calculations above, an approximation of between 5 and 11 μg rhBMP-2/mg collagen matrix incorporates the range of dimensional orientations for a monolayer of rhBMP-2 molecules occupying the collagen matrix surface. This is assuming the ideal case where all available surface area is occupied by rhBMP-2.

High Limit of v : rhBMP-2 Saturation in the Free Volume inside the Collagen Cylinder. The theoretical free volume inside the collagen cylinder was approximated as the buffer volume that was typically transferred with a collagen cylinder to the sample. This buffer transfer volume, obtained primarily to assess the dilution effect to rhBMP-2 in the sample, was experimentally determined to be approximately $75.3 \mu\text{L}$ for a 4-mm collagen cylinder, or $9.9 \times 10^{-8} \text{ m}^3$ per mg of collagen matrix. With the published rhBMP-2 dimer dimensions of $70 \text{ \AA} \times 35 \text{ \AA} \times 30 \text{ \AA}$,²⁸ the rhBMP-2 dimer molecular volume was approximated to be $7.35 \times 10^{-26} \text{ m}^3$ per dimer. Therefore, the rhBMP-2 dimer saturation in the free volume inside the collagen matrix was theoretically estimated to be 1.35×10^{18} rhBMP-2 dimers per milligram of collagen matrix. By using Avogadro's number, this high-limit free volume saturation is 67.3 mg rhBMP-2 per milligram of collagen cylinder, as compared to the low-limit surface saturation of 5 to 11 μg rhBMP-2 per milligram of collagen matrix.

Equilibrium Binding of rhBMP-2 to a Collagen Matrix.

To experimentally evaluate the binding strength and type of binding (monolayer versus multilayer) between rhBMP-2 and a collagen delivery matrix, an equilibrium study was performed. Kinetic experiments established the minimum time

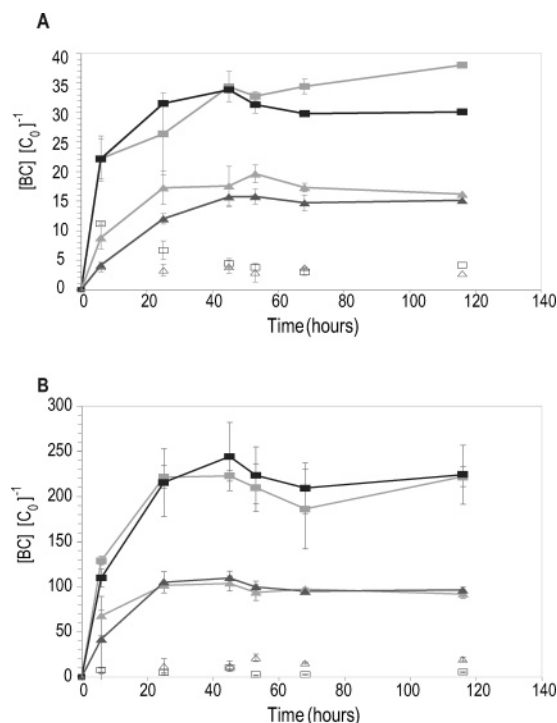


Figure 2. (A) Binding kinetics at $17 \mu\text{g/mL}$ initial rhBMP-2 concentration. The y-axis represents bound $\mu\text{g/mL}$ rhBMP-2 per mg/mL collagen matrix or bound μg rhBMP-2/mg collagen. (B) Binding kinetics at $730 \mu\text{g/mL}$ initial rhBMP-2 concentration in pH 5.4, 25 mM NaCl with 3 and 4 mm collagen cylinders, respectively (black and gray squares, respectively); pH 4.4 with no added NaCl with 3 and 4 mm collagen cylinders (black and gray triangles, respectively); controls in pH 5.4, 25 mM NaCl in the absence of collagen (open squares) and in pH 4.4 with no added NaCl in the absence of collagen (open triangles).

for binding equilibrium between rhBMP-2 and a collagen matrix, at extreme buffer conditions. Binding equilibrium at extreme rhBMP-2 concentrations (17 and 730 $\mu\text{g/mL}$) in high pH and high NaCl buffer (pH 5.4, 25 mM NaCl) and in low pH and low NaCl buffer (pH 4.4, no added NaCl) occurred at approximately 50 h as shown in Figure 2. (pH of 5.4 in 5 mM L-glutamic acid was the highest pH employed where rhBMP-2 remains soluble at the concentrations of rhBMP-2 and NaCl used in these experiments.) The mass of rhBMP-2 bound per milligram of collagen was equal in the 3-mm and 4-mm collagen matrix cylinders, indicating that saturation in the 4-mm collagen cylinder was not limited by the rhBMP-2 mass in the sample.

Table 1 shows that at pH 4.4 the binding saturation, v , increased between the buffer with no added NaCl and the buffer with 12 mM NaCl, but appeared to plateau at 12 mM NaCl with little change between 12 mM and 25 mM NaCl. Similar saturation plateaus at 12 mM and 25 mM NaCl were observed for samples at pH 4.9 and 5.4.

As shown in Table 1, the apparent equilibrium binding constant, K_b , tended to increase with increasing pH, but K_b did not tend to increase with increasing NaCl. Examination of the apparent standard free energy of interactions showed the same trend. Binding was more favorable at pH 5.4 than at pH 4.4 (see Table 1). The K_b values were obtained as the slope of the visual best fit of a single line or two tangent lines to the data points shown in Figure 3A–C. An approximate K_b error can be assessed as the variability in the visual best fit of tangent lines to the data points in Figure 3A–C, taking the relative error bars of the data points into consideration. In the present

Table 1. Binding Strength of Unfractionated rhBMP-2 to Collagen

pH	NaCl mM	ν or ν_T^a $\mu\text{g}/\text{mg}$	K_b or K_{b1}^b (M^{-1})	app $\Delta G_1^{\circ c}$ kcal mol^{-1}	K_{b2}^d (M^{-1})	app $\Delta G_2^{\circ c}$ kcal mol^{-1}
4.4	none added	80	6.6×10^3	-5.19	N.D. ^e	<i>f</i>
4.4	12	170	5.4×10^3	-5.08	N.D.	
4.4	25	140	6.3×10^3	-5.18	N.D.	
4.9	none added	110	2.4×10^4	-5.94	N.D.	
4.9	12	260	2.6×10^4	-6.02	8.4×10^3	-5.35
4.9	25	260	2.3×10^4	-5.95	1.0×10^4	-5.45
5.4	none added	150	6.3×10^4	-6.54	1.2×10^4	-5.56
5.4	12	260	4.3×10^4	-6.32	8.1×10^3	-5.33
5.4	25	260	7.8×10^4	-6.67	9.0×10^3	-5.39

^a ν_T is the total number of binding sites per unit of substrate (collagen) for biphasic binding (where two or more modes of binding are observed by a nonlinear Scatchard plot), comparable to ν for simple binding (determined from the x-intercept of Scatchard plots where one mode of binding is observed as a linear Scatchard plot). ^b K_b or K_{b1} is the equilibrium binding constant of rhBMP-2 to collagen matrix determined from slope of linear trend line of Scatchard plots. ^c ΔG_1° and ΔG_2° are the apparent standard free energies for observed monophasic and biphasic interaction between rhBMP-2 and collagen matrix at 25 °C, where $\Delta G^{\circ} = -RT \ln K_b$. ^d K_{b2} = equilibrium binding constant determined from trend line of final portion of data in a nonlinear Scatchard plot. ^e N.D. represents those Scatchard plots that were linear, and therefore, biphasic interaction was not detected. ^f Data points in respective Scatchard plots were deemed too scattered to generate a slope and determine a binding constant.

Table 2. rhBMP-2 Isoforms Binding to Collagen Matrix

isoform	pH	NaCl mM	ν or ν_T^a $\mu\text{g}/\text{mg}$	K_b or K_{b1}^b (M^{-1})	app $\Delta G_1^{\circ c}$ kcal mol^{-1}	K_{b2}^d (M^{-1})	app $\Delta G_2^{\circ c}$ kcal mol^{-1}
<Q ₂₈₃ /Q ₂₈₃	4.4	none added	40	<i>e</i>			
<Q ₂₈₃ /Q ₂₈₃	4.4	25	140	2.5×10^4	-5.99	4.8×10^3	-5.02
<Q ₂₈₃ /Q ₂₈₃	5.4	none added	60				
<Q ₂₈₃ /Q ₂₈₃	5.4	25	120	9.9×10^4	-6.81	9.0×10^3	-5.39
T ₂₆₆ /T ₂₆₆	4.4	none added					
T ₂₆₆ /T ₂₆₆	4.4	25	30				
T ₂₆₆ /T ₂₆₆	5.4	none added	60				
T ₂₆₆ /T ₂₆₆	5.4	25	210	7.2×10^4	-6.62	9.6×10^3	-5.43

^a ν_T is the total number of binding sites per unit of substrate (collagen) for biphasic binding (where two or more modes of binding are observed by a nonlinear Scatchard and is comparable to ν for simple binding (determined from the x-intercept of Scatchard plots where one mode of binding is observed as a linear Scatchard plot). ^b K_b or K_{b1} is the equilibrium binding constant for rhBMP-2 interaction with the collagen matrix, as determined from the slope of linear trend line of Scatchard plots. ^c apparent standard free energy of interaction for rhBMP-2 and collagen matrix at 25 °C, where $\Delta G^{\circ} = -RT \ln K_b$. ^d K_{b2} = equilibrium binding constant determined from trend line of final portion of data in a nonlinear Scatchard plot. ^e For entries with no data recorded, data points in respective Scatchard plots were deemed too scattered to generate a slope and determine a binding constant.

experiments, the focus was on the relative changes in K_b as a function of pH and NaCl, rather than on determining absolute K_b values. (The apparent errors in K_b and the calculated values of ΔG° of interaction presented in Tables 1–2 oscillated between 5% and 10% of the nominal values.)

As with increasing K_b , the change from a linear to a biphasic Scatchard plot (Figure 3A–C) tended to occur with increasing pH. The biphasic nature of binding at pH 4.9 was very slight (Figure 3B), while the biphasic nature of binding at pH 5.4 was more pronounced. Whether a binding curve should be described by a simple or a biphasic Scatchard plot depends on whether there is one or more than one mode of binding and on the disparity between the two K_b values representing the binding strengths of the first versus the subsequent modes of binding. As might be expected, at the higher pH conditions, the data appeared to fit a biphasic Scatchard plot (and therefore identify more than one mode of binding), the weaker binding, K_{b2} , was similar to the K_b values of binding described by a simple Scatchard plot at the lower pH. Overall, both binding saturation and the strength of binding increased at pH values of 4.9 and 5.4 as compared to pH 4.4 (Figure 3A–C).

Binding Strength of Purified rhBMP-2 Isoforms. The rhBMP-2 employed in these studies was a mixture of six different covalent dimers composed of various combinations of three different monomers. To dissect the potential contribution of the individual dimers to the overall binding of the hetero-

geneous (unfractionated) rhBMP-2, binding experiments were conducted with purified <Q₂₈₃/Q₂₈₃ and T₂₆₆/T₂₆₆ isoforms. These two isoforms were selected for the analysis because they show the most striking differences with respect to overall charge as shown by cation exchange chromatography (Figure 4). In addition, the N-terminal glutamine of other isoforms spontaneously cyclizes to pyroglutamic acid during the course of the binding experiments. Therefore, clear analysis of Q₂₈₃/Q₂₈₃, <Q₂₈₃/Q₂₈₃, and Q₂₈₃/T₂₆₆ binding to the collagen matrixes becomes experimentally complex.

At pH 4.4 in 25 mM NaCl, the <Q₂₈₃/Q₂₈₃ isoform binding to the collagen matrix followed a biphasic binding isotherm and similar binding saturation (ν) to heterogeneous rhBMP-2 at the same pH and NaCl concentration (Figure 5A). At pH 4.4 in the absence of NaCl, the <Q₂₈₃/Q₂₈₃ isoform showed almost no binding. Since the Scatchard plot (Figure 5B) showed no definitive slope for this small amount of binding, an approximate saturation value of 40 μg rhBMP-2/mg collagen was estimated from the binding isotherm (Figure 5A).

Table 2 shows a summary of K_b and ν parameters for binding in 25 mM NaCl (as determined from Scatchard plots) and the ν parameter for binding in the absence of NaCl as estimated from the binding isotherm. At pH 5.4 in 25 mM NaCl, <Q₂₈₃/Q₂₈₃ binding was shown to be biphasic by the Scatchard plot analysis (Figure 6). At pH 5.4 in the absence of NaCl, the <Q₂₈₃/Q₂₈₃ binding was similar (almost no binding) to binding at

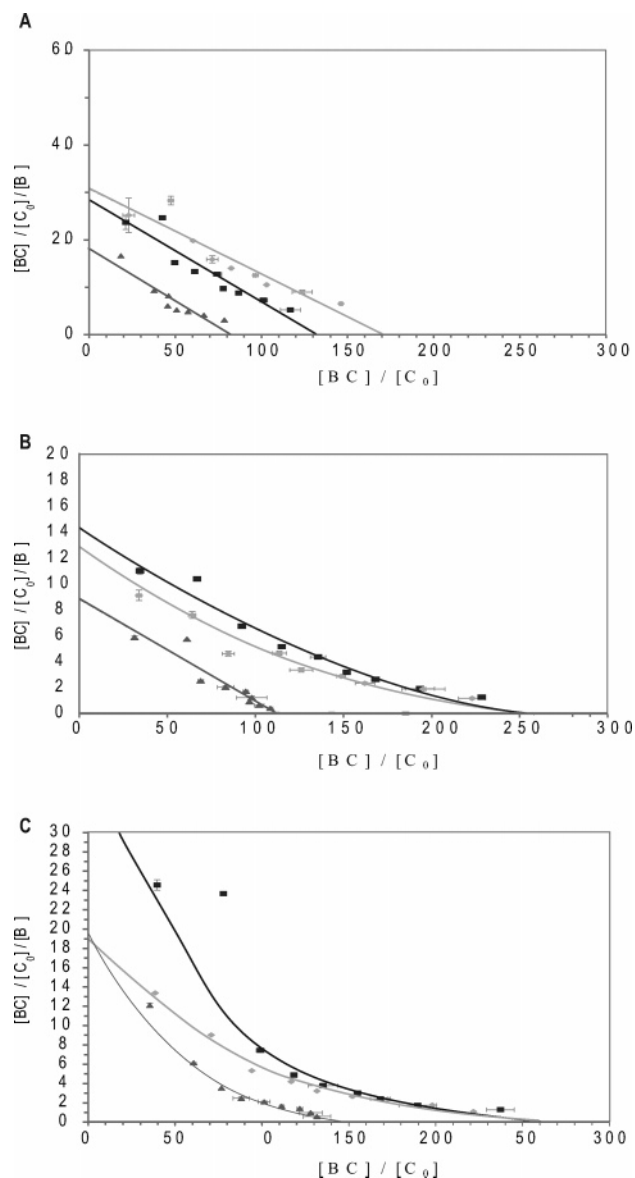


Figure 3. (A) Scatchard plots of rhBMP-2 binding to collagen at pH 4.4 either in buffer containing no added NaCl (black triangles), 12 mM NaCl (gray diamonds), or 25 mM NaCl (black squares). The x-axis $[BC]/[C_0]$ represents $\mu\text{g/mL}$ rhBMP-2 bound per mg/mL collagen. The y-axis $[BC]/[C_0]/[B]$ is $\mu\text{g/mL}$ rhBMP-2 bound per mg/mL collagen per $\mu\text{g/mL}$ free rhBMP-2. (B) Scatchard plots of rhBMP-2 binding to collagen at pH 4.9 in the absence of NaCl (black triangles), 12 mM NaCl (gray squares), and 25 mM NaCl (black squares). (C) Scatchard plots of rhBMP-2 binding to collagen at pH 5.4 in buffer containing either no added NaCl (black triangles), 12 mM NaCl (gray diamonds), or 25 mM NaCl (black squares) at pH 5.4. The lines are trends through the data points.

pH 4.4 without added NaCl. Binding saturation at these conditions was not obtainable from the Scatchard plot because of scatter of the data points. Table 2 shows a summary of the obtainable binding parameters.

Binding of T_{266}/T_{266} isoforms to the collagen matrix at pH 4.4 in the absence of NaCl was negligible. Estimation of parameters for binding in the absence of NaCl was not feasible, except for the binding saturation parameter, ν , which was approximated as 25 μg rhBMP-2 bound per milligram of collagen from the binding isotherm analysis (Table 2). At pH 5.4 in the absence of NaCl, there was almost no binding of the T_{266}/T_{266} isoform to the collagen matrix. The binding saturation was estimated at 60 $\mu\text{g}/\text{mg}$ of collagen from the binding

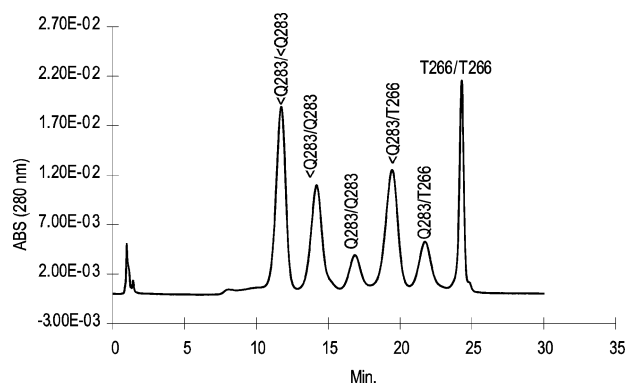


Figure 4. Typical cation exchange-HPLC profile of dimeric rhBMP-2 showing the isoform distribution. The rhBMP-2 isoforms were fractionated following a published procedure.²⁶ Briefly, an estimated 35 μg of rhBMP-2 from each sample or control was injected over a cation exchange column (Pharmacia Mono S, 5.0 mm \times 50 mm) at 1 mL/min for 30 min. At the beginning of the run, the mobile phase was held constant at 85% A (20 mM sodium acetate and 10% acetonitrile in deionized H_2O at pH 5.0) and 15% B (20 mM sodium acetate, 1.5 M NaCl, and 10% acetonitrile in deionized H_2O at pH 5.0). The percent B was increased linearly from 15% at 6 min to 38% at 7 min, then linearly to 40% B at 10 min, then linearly to 54% at 18 min, then linearly to 70% at 19 min, then held constant until 23 min, then decreased linearly to 15% at 24 min, and then held constant until the end of the run at 30 min.

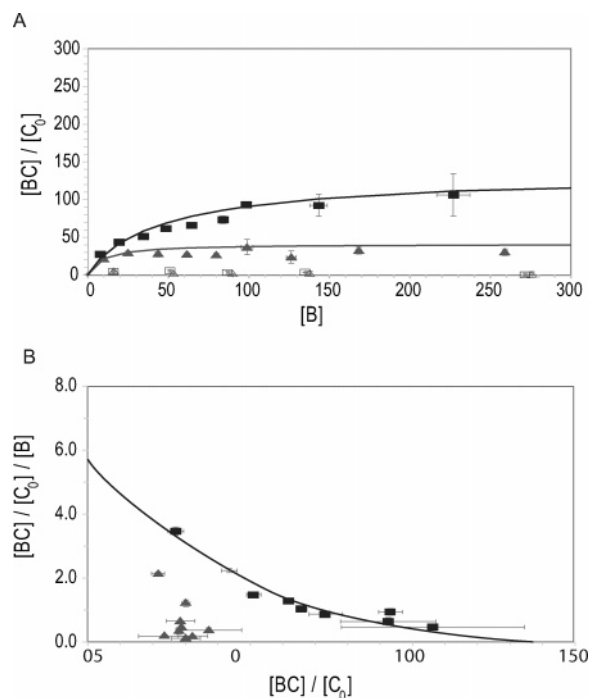


Figure 5. (A) Binding isotherms for the rhBMP-2 $<Q/<Q$ isoform to collagen in 5 mM glutamic acid buffer at pH 4.4 either in the absence of NaCl (black triangles) or in 25 mM NaCl (black squares). Open squares and triangles represent rhBMP-2 binding in the absence of collagen. The lines are fitted curves. (B) Scatchard plots of the rhBMP-2 $<Q/<Q$ isoform binding to collagen in 5 mM glutamic acid buffer at pH 4.4 either in the absence of NaCl (black triangles) or 25 mM NaCl (black squares). The lines are trends through the data points. The x- and y-axes are as described in Figure 3.

isotherm, similar to binding of the $<Q_{283}/<Q_{283}$ isoform at pH 5.4 in the absence of NaCl. Binding of T_{266}/T_{266} isoforms at pH 5.4 in 25 mM NaCl had a higher ν relative to binding at pH 4.4 (Table 2) and appeared biphasic by the Scatchard plot analysis.

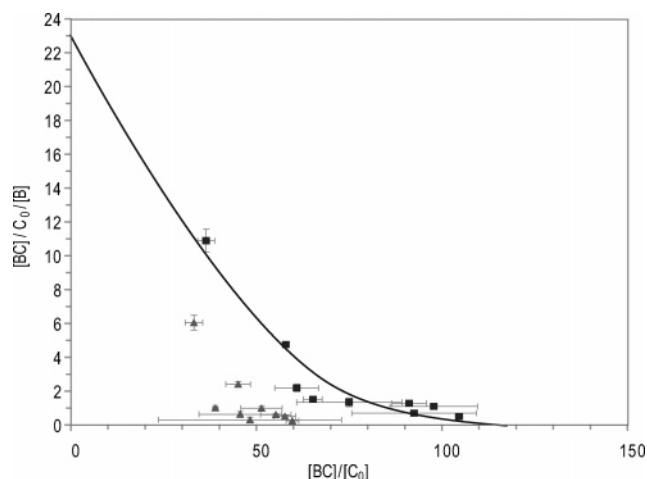


Figure 6. Scatchard plots for the binding of rhBMP-2 $\langle Q_{283}/\langle Q_{283}$ isoform to collagen in 5 mM glutamic acid buffer at pH 5.4 in either no added NaCl (gray triangles) or 25 mM NaCl (black squares). See Figure 3 for a description of the x- and y-axes.

Discussion

The type and strength of association between therapeutic proteins and their delivery systems should be established early in the research and development process to allow optimization of the pharmacokinetic and pharmacodynamic profiles of drug candidates. Kinetic and thermodynamic analysis of the interactions between rhBMP-2 and the collagen matrix suggest that the association is specific and not a consequence of adsorption or aggregation caused by the matrix or solution conditions. The rhBMP-2/collagen association reaches an equilibrium that changes on the basis of the rhBMP-2 isoform content, on pH, and, to a lesser extent, on ionic strength.

As shown in the Results section, on the basis of the molecular dimensions of rhBMP-2 and prior collagen surface analysis determination,²⁶ monolayer saturation of rhBMP-2 should form at approximately 5–11 μg rhBMP-2/mg collagen matrix and total volume saturation of rhBMP-2 should occur at ~ 67.3 mg rhBMP-2/mg collagen matrix. In addition, we can estimate that the maximum monolayer saturation plus entrapment of the rhBMP-2 mass in the free volume of the matrix is 85 μg rhBMP-2 trapped and/or bound within the matrix. (The nominal rhBMP-2 mass in the free volume of collagen matrix is approximated to be 74 μg rhBMP-2/mg collagen matrix, where the concentrations inside and outside the matrix are equal at 750 μg rhBMP-2/mL, and a 4-mm collagen cylinder contains 0.76 mg of collagen and 75.3 μL of inner volume.)

Yet, the binding experiments yielded ν values up to 250 μg rhBMP-2/mg collagen, as shown in Tables 1–2 and Figures 2, 3, 5, and 6. This exceeds a dense monolayer by up to 24-fold and exceeds a monolayer plus entrapment by nearly 3-fold. Thus, the observed binding saturation values described (see Tables 1–2 and Figures 2, 3, 5, and 6) constitute at least multilayers of rhBMP-2 on the collagen surface. Experiments conducted in different buffers showed that the number of layers fluctuates with ionic strength (NaCl) and, in some cases, pH, reaching the maximum of approximately 250 μg rhBMP-2 bound per milligram collagen.

The discrepancy between the trends of $\langle Q_{283}/\langle Q_{283}$ binding saturation versus heterogeneous rhBMP-2 and T_{266}/T_{266} isoforms suggest that the T_{266}/T_{266} isoform does not contribute to the formation of the multilayer at pH 4.4. As the NaCl concentration increases, more of the $\langle Q_{283}/\langle Q_{283}$ isoform enters into the multilayer formation. The increase in pH led the T_{266}/T_{266}

isoform to enter into the multilayer formation, with the consequential effect of increasing the overall binding saturation. The increase in binding saturation of the $\langle Q_{283}/\langle Q_{283}$ isoform as a function of NaCl concentration may be caused by intrachain salt bridges or hydrophobic interactions between rhBMP-2 molecules in the multilayer.

Ionic and Hydrophobic Interactions. The $\langle Q_{283}/\langle Q_{283}$ isoform binding saturation, ν , is a function of ionic strength as shown by the dependence on NaCl concentration (see Figures 5 and 6), while the unfractionated rhBMP-2 and T_{266}/T_{266} isoform binding saturation increases with both NaCl concentration and increasing pH. The binding affinity K_b was shown to be a function of pH and not of NaCl concentration. One simple possible explanation for these results is that the observed biphasic nature of binding between rhBMP-2 and the collagen matrix is the result of a mixture of interacting forces between rhBMP-2 molecules in the multilayer formation, including hydrophobic and ionic interactions. At pH 4.4 in the absence of NaCl (low ionic strength), hydrophobic interactions between rhBMP-2 molecules in the multilayer formation could dominate. The T_{266}/T_{266} isoform of rhBMP-2 is more positively charged than $\langle Q_{283}/\langle Q_{283}$ isoforms (because of the N-terminal basic core extension), hence it might not contribute to the multilayer formation. At pH 4.4 in 25 mM NaCl, hydrophobic interactions could still dominate the interactions in the multilayer, and the T_{266}/T_{266} isoform might not contribute to the multilayer form of interaction with the collagen matrix. However, the increase in ionic strength induced by NaCl allows for more hydrophobic interactions between $\langle Q_{283}/\langle Q_{283}$ isoforms in the multilayer formation. While more $\langle Q_{283}/\langle Q_{283}$ dimeric molecules contribute to the multilayer formation in high ionic strength than in low ionic strength buffer, i.e., in the absence of NaCl, the overall binding strength between molecules in the multilayer formation remained constant.

At pH 5.4 in low ionic strength buffer (no added NaCl), the T_{266}/T_{266} isoform contributes to a small degree to rhBMP-2 multilayer formation on the collagen matrix. This might be a manifestation of some loss in the positive charge on the N-terminus of the T_{266}/T_{266} isoform, as the pH is moving toward the direction of its isoelectric point of approximately pH 9. On the other hand, the $\langle Q_{283}/\langle Q_{283}$ isoform also becomes more negatively charged and contributes to ionic binding in the multilayer formation. The $\langle Q_{283}/\langle Q_{283}$ and T_{266}/T_{266} isoforms therefore may bind in a multilayer fashion to the collagen matrix with a combination of ionic and hydrophobic interactions. At pH 5.4 at 25 mM NaCl, the T_{266}/T_{266} isoform contribution to the overall multilayer binding is significant on account of an increased availability of free ions in the aqueous environment for salt bridges, allowing therefore multilayer formation of T_{266}/T_{266} upon binding to the collagen matrix. Hence, both increased binding saturation and increased binding affinity are observed.

The general trend of the “binding” studies performed by Friess et al.²⁰ is similar to our studies, i.e., the $\langle Q_{283}/\langle Q_{283}$ isoform appears to show higher “binding”/retention to a collagen matrix than the T_{266}/T_{266} isoform. Nevertheless, the total apparent amounts of isoforms bound to collagen are different. This difference might be explained by the fact that the prior study²⁰ is not measuring true thermodynamic binding of rhBMP-2 isoforms to the collagen delivery matrix. The procedure employed by the authors in the previous study²⁰ deduces binding from the fraction of rhBMP-2 that is squeezed out of the collagen sponge after loading the isoforms directly onto a naked sponge without any pretreatment and under nonequilibrium conditions. This could explain the quantitative differences in

binding between the present study and the reported study.²⁰ Also, the low volume loaded onto collagen matrixes in the prior study²⁰ (650 μ L onto 6.5 cm² collagen sponge pieces) probably made the concentration of any potential leachables from the collagen matrix a critical factor. These leachables could in turn affect the final binding of rhBMP-2 to the collagen matrix.

Nevertheless, our results are consistent with observations made by Abbatiello and Porter,²⁹ who reported that $<Q_{283}/<Q_{283}$ isoforms of rhBMP-2 are less soluble at pH values approaching physiological conditions and when the NaCl concentration approached 100 mM, consistent with an affinity precipitation mechanism that requires anion-dependent formation of protein complexes.²⁹ Although at the present time we are uncertain of the rhBMP-2 isoform distribution in vivo, it is interesting to note that the N-terminal basic amino acid core might play a role in the long-range biological action of rhBMP-2 by restricting ligand diffusion.^{30,31} Thus, the 17 basic amino acid N-terminal extension of T₂₆₆/T₂₆₆ could be perfectly positioned to serve that role. Conversely, the intrinsic higher propensity of $<Q_{283}/<Q_{283}$ isoforms to form multilayers compared with T₂₆₆/T₂₆₆ isoforms (Table 2) and the relationship between rhBMP-2 retention and efficacy⁹ suggest that the $<Q_{283}/<Q_{283}$ isoform is the potential in vivo predominant dimeric species retained by oligomerization at the target biological site.

Biphasic Scatchard Plots and Self-Association. While the pH and NaCl levels employed in these experiments were well below those used by Abbatiello and Porter,²⁹ their general observation that rhBMP-2 is less soluble with increasing pH and NaCl levels is consistent with oligomerization of rhBMP-2. Indeed, it has been shown that changes in rhBMP-2 solubility with pH are the physical manifestation of rhBMP-2 reversible self-association.³² Hence, the multilayer mode of interaction of rhBMP-2 with the collagen matrix may not be so much a consequence of rhBMP-2 interacting with collagen and the latter inducing additional binding sites in rhBMP-2 for multilayer formation, but rather self-association of rhBMP-2 due to its favorable intermolecular energetic, driven mainly by pH. Thus, the self-associated forms of rhBMP-2 will then bind to the collagen matrix resulting in the ligand, namely, rhBMP-2, interacting as a multilayer and reflected in a biphasic Scatchard plot. The contribution of protons to the linkage free energy of binding ($\Delta\Delta G^{\circ}_{\text{binding}} = \Delta G^{\circ}_{\text{pH}5.4} - \Delta G^{\circ}_{\text{pH}4.4}$) could be estimated from the data in Table 1 as ~ 1.35 kcal mol⁻¹. By contrast, ionic strength appears to have a minor effect on the energetics of rhBMP-2 collagen interactions. The contribution of NaCl to the apparent linkage free energy is only ~ 0.13 kcal mol⁻¹.

It is unknown whether a true monomer-multimer equilibrium exists on the surface of the collagen matrix or a continuous multilayer formation. The present study does not distinguish the sequence of events leading to multilayer formation by rhBMP-2 on the surface of the collagen delivery matrix. However, sedimentation velocity analyses have shown the formation of discrete and reversible rhBMP-2 oligomers (10–11S self-associated species) in solution depending on isoform composition and pH.³² This suggests a potential equilibrium between nonassociated and associated rhBMP-2 forms whose distribution is modulated by solution conditions. Thus, oligomerization of rhBMP-2³² or the multilayering observed on the surface of collagen matrixes might be critical in vivo to maximize biological efficacy. Rabbit ulna osteotomy models have shown clearly the need for a collagen delivery system to retain rhBMP-2 at the target site and therefore obtain optimal efficacy.^{9,33} Nevertheless, different anatomical sites might require different kinetics of rhBMP-2 release for optimal

performance. Thus, solution variables that could modulate the energetics of interaction between rhBMP-2 and the delivery system could help in identifying the desired pharmacokinetic profile.

Conclusion

The thermodynamic approach in this analysis could be applicable to address and assess formulation parameters for drug products delivered by a vehicle such as a collagen matrix. These findings suggest that increasing mainly the pH in the formulation could optimize the amount of rhBMP-2 delivered by the collagen matrix to the site of interest. It is likely that proton ions both induce and facilitate the self-association of rhBMP-2 to form a multilayer at the surface of the collagen matrix. The biphasic nature of the Scatchard plots is consistent with self-association, as has been shown for other systems.³⁴

Acknowledgment. We thank the NIH (EB002520 and EB003210) for support of various aspects of this work.

References and Notes

- (1) Ratner, B. D.; Hoffman, A. S.; Schoen, F. J. In *Biomaterials Science: an Introduction to Materials in Medicine*; Academic Press: New York, 1996; pp 88–92.
- (2) Friess, W. Doctoral dissertation. Friedrich-Alexander-Universität Erlangen-Nürnberg, Germany, 2000.
- (3) Singh, M. Doctoral dissertation. University of Maryland, 2004.
- (4) Singh, M.; Lumpkin, J. A.; Rosenblatt, J. J. *Controlled Release* **1995**, 35, 165–179.
- (5) Marks, M. G.; Doillon, C.; Silver, F. H. *J. Biomed. Mater. Res.* **1991**, 25, 683–696.
- (6) Uludag, H.; D'Augusta, D.; Golden, J.; Li, J.; Timony, G.; Riedel, R.; Wozney, J. M. *J. Biomed. Mater. Res.* **2000**, 50 (2), 227–238.
- (7) Uludag, H.; D'Augusta, D.; Palmer, R.; Timony, G.; Wozney, J. J. *Biomed. Mater. Res.* **1999**, 46, 193–202.
- (8) Winn, S. R.; Uludag, H.; Hollinger, J. O. *Clin. Orthoped.* **1999**, 367S, S95–106.
- (9) Geiger, M.; Li, R. H.; Friess, W. *Adv. Drug Deliv. Rev.* **2003**, 55, 1613–1629.
- (10) Urist, M. R. In *Bone morphogenetic proteins: biology, biochemistry and reconstructive surgery*; Lindholm, T. S., Ed.; R. G. Landes Company: Austin, TX, 1996; pp 7–27.
- (11) Karageorgiou, V.; Meinel, L.; Hofmann, S.; Malhotra, A.; Volloch, V.; Kaplan, D. J. *Biomed. Mater. Res., A* **2004**, 71, 528–37.
- (12) Meinel, L.; Hofmann, S.; Karageorgiou, V.; Zichner, L.; Langer, R.; Kaplan, D.; Vunjak-Novakovic, G. *Biotechnol. Bioeng.* **2004**, 379–91.
- (13) Porter, T. J.; Rathore, S.; Rouse, J.; Denton, M. *J. ASTM Int.* **2004**, 1, 1–21.
- (14) Uludag, H.; Friess, W.; Williams, D.; Porter, T.; Timony, G.; D'Augusta, D.; Blake, C.; Palmer, R.; Biron, B.; Wozney, J. *Ann. N. Y. Acad. Sci.* **1999**, 875, 369–378.
- (15) Lecanda, F.; Avioli, V.; Cheng, S. *J. Cell Biochem.* **1997**, 67, 386–398.
- (16) Burg, K. J. L.; Porter, S.; Kellan, J. F. *Biomaterials* **2000**, 21, 2347–2359.
- (17) Kirker-Head, C. A. *Adv. Drug Deliv. Rev.* **2000**, 43, 65–92.
- (18) Brekke, J. H.; Toth, J. M. *J. Biomed. Mater. Res.* **1998**, 43, 380–398.
- (19) Friess, W.; Uludag, H.; Foskett, S.; Biron, R. *Pharm. Dev. Technol.* **1999**, 4, 387–396.
- (20) Friess, W.; Uludag, H.; Foskett, S.; Biron, R. *Int. J. Pharm.* **1999**, 185, 51–60.
- (21) Zhu, Y.; Oganessian, A.; Keene, D. R.; Sandell, L. J. *J. Cell Biol.* **1999**, 144, 1069–1080.
- (22) Boix, T.; Gomez-Morales, J.; Torrent-Burgues, J.; Monfort, A.; Puigdomenech, P.; Rodríguez-Clemente, R. *J. Inorg. Biochem.* **2005**, 99, 1043–1050.
- (23) Israel, D. I.; Nove, J.; Kerns, K. M.; Moutsatsos, I. K.; Kaufman, R. *J. Growth Factor* **1996**, 13, 139–150.
- (24) Friess, W.; Lee, G.; *Biomaterials*. **1996** 17, 2289–2294.

- (25) Walker, T. A.; Ho, T. V.; Akbari, N. *J. Liq. Chromatogr.* **1989**, *12*, 1213.
- (26) Morin, R. M.S. Thesis. Tufts University, Medford, MA, 2001.
- (27) Rathore, S.; Hammerstone, K. M.; Dansereau, S.; Porter, T. J. *Protein Sci.* **1995**, *4* (Suppl. 2), 110 (443S).
- (28) Scheufler, C.; Sebal, W.; Hulsmeyer, M. *J. Mol. Biol.* **1999**, *287*, 103–115.
- (29) Abbatiello, S. E.; Porter, T. J. *Protein Sci.* **1997**, *6*, 99.
- (30) Jones, C. M.; Armes, N.; Smith, J. C. *Curr. Biol.* **1996**, *6*, 1468–1475.
- (31) Ohkawara, B.; Lemura, S.; ten Dijke, P. *Curr. Biol.* **2002**, *12*, 205–209.
- (32) Perez-Ramirez, B.; Steckert, J. In *Therapeutic Proteins: Methods and Protocols*; Smales, C. M., James, D. C., Eds.; Humana Press: Totowa, NJ, 2005; Vol. 308, Chapter 24, pp 301–318.
- (33) Li, R. H.; Wozney, J. *Trends Biotechnol.* **2001**, *19* (7), 255–256.
- (34) Andreu, J. M.; Na, G. C.; Timasheff, S. N. *Pharmacol. Ther.* **1991**, *52*, 191–210.

BM050461I